Late Holocene floodplain development, land-use, and hydroclimate-flood relationships on the lower Ohio River, USA

[1]Broxton W. Bird, [2]Robert C. Barr, [3]Julie Commerford, [1]William P. Gilhooly III, [4]Jeremy J. Wilson, [5]Bruce Finney, [6]Kendra McLauchlan, and [4]G. William Monaghan

[1]Department of Earth Sciences, Indiana University-Purdue University, Indianapolis, IN 46202
[2]Center for Earth and Environmental Sciences, Indiana University-Purdue University, Indianapolis, IN 46202
[3]Department of Geography, Saginaw Valley State University, University Center, MI 48710
[4]Department of Anthropology, Indiana University-Purdue University, Indianapolis, IN 46202
[5]Departments of Biological Sciences and Geosciences, Idaho State University, Pocatello, ID 83209
[6]Department of Geography, Kansas State University, Manhattan, KS 66506

Abstract

Floodplain development, land-use, and flooding on the lower Ohio River are investigated with a 3,100-year-long sediment archive from Avery Lake, a swale lake on the Black Bottom floodplain in southern Illinois, USA. Twelve radiocarbon dates show that Avery formed at 1130 BCE (3100 cal yr BP), almost 3000 years later than previously thought, indicating that the Black Bottom floodplain is younger and more dynamic than previously estimated. Three subsequent periods of extensive land clearance were identified by changes in pollen composition, corresponding to Native American occupations before 1500 CE and the current Euro-American occupation

This is the author's manuscript of the article published in final edited form as:
Bird, B. W., Barr, R. C., Commerford, J., Gilhooly, W. P., Wilson, J. J., Finney, B., … Monaghan, G. W. (2019). Late-Holocene floodplain development, land-use, and hydroclimate–flood relationships on the lower Ohio River, US. The Holocene, 0959683619865598. https://doi.org/10.1177/0959683619865598

beginning in the 18th century. Sedimentation rates prior to 1830 CE changed independently of land clearance events, suggesting natural as opposed to land-use controls. Comparison with high-resolution paleoclimate data from Martin Lake, IN, indicates that lower Ohio River flooding was greatest when cold-season precipitation originating from the Pacific/Arctic predominated during positive Pacific North American (PNA) and Pacific Decadal Oscillation (PDO) mean states (1130 BCE to 2350 CE and 1150-1830 CE), but was reduced when warm-season precipitation from the Gulf of Mexico prevailed during negative PNA and PDO mean states (350 and 1150 CE). This flood dynamic was fundamentally altered for the lower Ohio River after 1830 CE despite a shift to negative PNA and PDO mean states by extensive land clearance, which increased warm-season runoff by reducing interception, infiltration, and evapotranspiration. Predicted increases in average precipitation and extreme rainfall events across the Midcontinental US are likely to perpetuate current trends toward more frequent and longer duration flood events because anthropogenic modifications have made the landscape less resilient to changing hydroclimatic conditions.

Key Words

Paleoclimate, Fluvial Dynamics, Floodplain Lakes, Anthropogenic Environmental Impacts, Sedimentology, Geochemistry, Pacific North American Mode, Pacific Decadal Oscillation

Introduction

The dynamic interaction between fluvial, climatic, and human systems has been studied by geomorphologists for several decades, with important implications for society (Knox, 1983, 2000, 2006; Bridge, 2009; Robinson, 2013). Extreme fluvial hydrologic events such as large

floods, as well as mean state changes in fluvial dynamics (e.g., average bank full discharge, landscape erosion, lateral mobility, and sediment concentrations) in response to climate variability, can profoundly affect fluvial landscapes, communities, and infrastructure. Recent increases in the duration and frequency of floods across the Midwest United States over the last few decades have occurred within the context of a 30% increase in mean annual precipitation (~75% of which occurs during the warm season) and more frequent, high-intensity rainstorm events (Pryor et al., 2014; Mallakpour and Villarini, 2015). At the same time, some fluvial systems have become more mobile, with large lateral migrations that have resulted in considerable damage to communities, infrastructure, and agricultural lands on the one hand, and the construction of new floodplains on the other (Robinson, 2013; Smith and Katz, 2013). In light of continued increases in average precipitation and extreme rainfall events, it is important to determine if recent fluvial-climate relationships represent a new dynamic related to hydrologic changes induced by land-use changes during the last ~200 years (i.e., conversion to agricultural and urban landscapes) or if they are within the range experienced in past climate-fluvial dynamics (Fitzpatrick et al., 1999; Fitzpatrick and Knox, 2000; Knox, 2006).

Characterizing past fluvial-climate dynamics is difficult because continuous, well-dated records of Midwest river dynamics, including flooding and floodplain construction, are scarce (Knox 2000). Likewise, high-resolution paleoclimate records from the Midwest that isolate hydroclimatic signals are rare. Seminal work in the Upper Mississippi River Valley (UMV) (Knox, 1984, 1985, 1987, 2000) used radiocarbon-dated paleochannels to show that bank full (1.56 yr floods) and large overbank flood events in UMV varied during the Holocene in ways that strongly suggest climatic linkages. Mechanistically, Knox (2000) suggested that paleo-floods within large and small fluvial systems were caused by increased warm-season

precipitation that originated from the Gulf of Mexico. Conversely, periods of low flood frequency were dominated by more westerly and/or northerly flow. This mechanistic interpretation was largely based on modern Midwest climatology, where warm-season precipitation is dominant over winter precipitation (~75% versus ~25%, respectively), and the association between many of the largest modern floods and the occurrence of warm-season atmospheric river events originating from the Gulf of Mexico (Dirmeyer and Kinter III, 2010; Lavers and Villarini, 2013). Other work from the Midwest, including along the Ohio River (Alexander and Nunnally, 1972; Stafford, 2004; Counts et al., 2015) and White River in Indiana (Herrmann and Monaghan, 2018) also shows variability in floodplain construction and the accumulation of floodplain alluvium that further suggests a connection between Holocene fluvial dynamics and climatic variability. Although climate is accepted as a likely driver of floodplain construction, the nature and timing of floodplain construction on large Midwest streams like the Ohio River is not resolved. Some studies suggest that large point bar systems on the lower Ohio River rapidly evolved over the last ~2000 thousand years (Counts et al., 2015) whereas others have concluded that they have been in a dynamic equilibrium for much of the Holocene (e.g., the Black Bottom; Alexander and Nunnally, 1972; Stafford, 2004).

Assessing the timing of floodplain construction and role of climate (and atmospheric circulation specifically) in driving past Midwest fluvial dynamics is difficult because paleo-records that isolated hydroclimatic conditions and atmospheric circulation were not available from the region until recently. Initially past Midwest hydroclimatic and atmospheric circulation changes were largely inferred indirectly from ecotonal shifts preserved in the regional network of pollen records and hydrologic variability recorded in lake and bog sediment records (e.g., Bartlein et al., 1984; Laird et al., 1998; Monaghan and Lovis, 2005; Booth et al., 2006). Other

studies applied isotope-based approaches to infer Holocene atmospheric circulation trends, but they were generally limited by either low temporal resolutions, which precluded all but broad-based comparisons with fluvial records, or by additional hydrologic influences, such as evaporation, which only allowed for indirect inferences of atmospheric circulation (Denniston et al., 1999; Liu et al., 2014a; Liu et al., 2014b). Recently published multi-proxy data ($\delta^{18}O_{calcite}$, $\delta^{13}C_{calcite}$, and %lithics) from Martin Lake, IN, however, provide direct information about moisture source variability (i.e., the Gulf of Mexico vs the Pacific/Arctic) and precipitation seasonality during the last two millennia at sub-decadal timescales (Bird et al., 2017b). With sufficiently temporally resolved and well-dated records of floodplain processes (e.g., floodplain construction, vertical alluvial accretion, and flooding), it is now possible to begin to investigate the extent to which climate influenced fluvial dynamics.

In addition to climate, questions remain about the role that human landscape modifications have played in modern Midwest fluvial dynamics. Research in the upper UMV has shown that landscape erosion and floodplain accretion increased significantly after the 1800s in response to widespread deforestation and landscape conversion to agricultural fields and urban centers (Fitzpatrick et al., 1999; Fitzpatrick and Knox, 2000; Knox, 2006; Munoz et al., 2018). These landscape changes increased fluvial sensitivity and flooding in response by decreasing interception and infiltration and increasing runoff and erosion. The observation that modern land-use altered runoff, increased flood sensitivities, and changed flood dynamics raises questions as to whether or not modern flood dynamics and their responses to warm-season precipitation changes are consistent with those in the past, or if flood-climate dynamics prior to large-scale land clearance were fundamentally different. Observations of the past relationships

between land-use and flood dynamics would help clarify the relative roles of land-use and climate in determining fluvial dynamics.

To investigate modern and paleo fluvial dynamics and their relationships with climate and land-use, we present a 3,100-year-long, high-resolution lake sediment archive from Avery Lake, IL, a small floodplain lake located on the lower Ohio River. The timing of floodplain construction was identified with basal radiocarbon dates while changes in flood occurrence were interpreted from sedimentation rate variations constrained by high-resolution radiocarbon dating and by variations in sedimentological and geochemical proxies of landscape erosion (e.g., magnetic susceptibility, titanium and zirconium abundances, grain size). Potentially obfuscating impacts of local land-use on the flooding reconstruction were evaluated by comparison with proxies of human landscape disturbance (pollen) and occupation (C, N, $\delta^{13}C$, $\delta^{15}N$, and Pb), which were additionally assessed in the context of extensive archaeological and historical occupation data from the Black Bottom. Lastly, climatic influences on floodplain construction and flooding were investigated by comparing the Avery Lake results with local and regional records of fluvial dynamics and climate.

Study Area: The Black Bottom and Avery Lake

Avery Lake (37.0788, -88.4906; 102 m above sea level; hereafter Avery) is located on the Black Bottom, a large crescent-shaped floodplain along the lower Ohio River in southern IL near the confluence with the Cumberland and Tennessee Rivers (Fig. 1). The Black Bottom floodplain measures approximately 16 by 5 km and is situated on the north side of a large meander loop point bar system in the Ohio River that is believed to have evolved over the last 10 to 20 thousand years, possibly in response to the rerouting of the ancestral Ohio River away from

the Cache Valley to the north (Alexander and Prior, 1968; Alexander and Nunnally, 1972). Progressive southward migration of the Ohio River deposited coarse point bar and natural levee sediments that were subsequently overlain by finer grained overbank and slack water deposits to form the modern-day floodplain (Alexander and Prior, 1971; Alexander and Nunnally, 1972). Morphologically, the Black Bottom is characterized by a series of ridges and swales that track the general trend of the meander loop, where the ridges are interpreted to represent former natural levees that lined paleo-channel banks and the swales mark the position of the ancestral Ohio River (Fig. 1) (Alexander and Prior, 1971).

Avery occupies a swale located approximately 1.6 km from the modern Ohio River channel. The lake is long and narrow (~90 m x 2.1 km) with a surface area of 0.13 km^2. Although its local watershed measures 15.8 km^2 (122:1 watershed to lake area ratio), it effectively becomes that of the Ohio River above the lake during floods (Fig. 1). The lake today has a uniform water depth of ~1 meter, as indicated by repeated depth measurements collected in the field along the lake's primary axis in June 2014 at the time of coring.

Flooding at Avery and the Black Bottom is generally influenced by the regional climate. Like much of the Midwest and Ohio River Basin, the modern climate is dominated by a warm-season precipitation maximum and cold-season precipitation minimum (approximately 75:25, respectively) (Bird et al., 2017b). Warm-season (April through October) precipitation is primarily delivered by southwest to northeast moving convective systems that derive their moisture from low-latitude sources like the Gulf of Mexico. This moisture is delivered deep into the midcontinental region by clockwise atmospheric circulation, resulting in Gulf moisture penetration as far north as the upper Midwest (Andresen et al., 2012). Occasionally, persistent south to north flow is established that results in anomalously large amounts of tropical moisture

being transported deep into the Midwest. These so-called atmospheric rivers are associated with significant positive precipitation anomalies that result in severe flooding (Dirmeyer and Kinter III, 2010; Lavers and Villarini, 2013). Cold-season (November through March) precipitation is generally derived from west to east moving frontal systems associated with a strengthened, often meridional, southerly displaced circumpolar jet stream. Although cold-season precipitation is considerably less than its warm-season counterpart, snowmelt floods are the most consistent source of flooding for larger midcontinental US river systems because widespread snow melt over large watershed areas is additive and produces significant discharge increases in trunk streams (Knox, 1988, 2000). Midwest snowmelt is also often associated with rain events, which contributes large stream discharges.

In order to distinguish between natural and anthropogenic drivers of the proxies measured on the Avery Lake sediment cores, it is essential to understand the anthropogenic land-use history of the Black Bottom. Since approximately 1800 CE, the Black Bottom has been largely utilized for agricultural purposes (mainly corn agriculture), although some residential structures are present. In the past, archaeologists have found evidence for a nearly 6,000 year long history of human presence on the landscape in close proximity to Avery (MacNeish, 1948; Butler, 2008) (Butler and Crow, 2013). Pre-Columbian Native American occupations on the Black Bottom were concentrated on the Black Bottom's floodplain ridges and most notably include the Kincaid Mounds site, which is immediately adjacent to Avery (Muller 1986). Three main periods of intensive occupation at and around Kincaid Mounds and Avery have thus far been identified: the Baumer, Lewis, and Mississippian phases. The Baumer phase is broadly dated to between 300 BCE and 300 CE and is associated with a circa 40 cm thick midden and associated refuse pits immediately adjacent to Avery (Butler and Welch, 2006). The Black Bottom was subsequently

unoccupied (or sparsely populated) between 300 and 600 CE, with the onset of Lewis phase habitation beginning between 600 and 650 CE and minimally lasting until 900 CE (Muller 1986). The Mississippian phase (1050 to 1400 CE) is the best-known and most studied occupation of the Black Bottom because large earthwork mounds, associated village, and extensive fortifications were constructed at Kincaid Mounds during this time (Fig. 1b) (Butler et al., 2011). The extent to which these Native American occupations impacted the ecology and landscape of the Black Bottom has not been systematically investigated to date. Doing so is important, however, because it is possible that natural (e.g., climatic) signals could be overwhelmed by local land-use changes. To overcome this potential complication, pollen analyses were used in conjunction with the geochemical and sedimentological analyses to assess relationships between land-use and other proxy variability.

Methods

Sample collection

Four continuous, 10-meter-long sediment cores were collected from two locations at Avery in June 2014 using a modified Livingstone piston corer driven by an electric winch coring tower system mounted on a floating raft (Wright et al., 1984). Overlapping Livingstone cores were offset by 50 cm at each location to ensure complete recovery. One-meter-long surface cores capturing the sediment-water interface were additionally collected for each of the Livingstone core locations using a modified piston corer. Cores were stored at 4˚C at the Indiana University-Purdue University, Indianapolis (IUPUI) Paleoclimatology and Sedimentology Laboratory prior to analysis. A composite sediment core measuring 995 cm was constructed by matching distinct

stratigraphic units and sedimentological measurements (magnetic susceptibility, total organic matter, and geochemistry from X-ray fluorescence). The composite core penetrated to 10.0 m depth, but the lowest 5 cm were lost during the coring process because they were composed of sand and gravel, which is difficult to retain with a modified Livingstone corer.

Sediment core processing, dry bulk density, loss on ignition, and magnetic susceptibility

Sediment cores were split into work and archive halves, photographed, described, and volumetrically sub-sampled (1 cm^3) at 2-cm intervals for dry bulk density (BD; g cm^{-3}) and loss-on-ignition (LOI) analysis. All samples were dried for 24 hours at 60ºC and reweighed to determine dry bulk density. Total organic matter (%TOM) and carbonate (%TC) abundances were determined by LOI after combustion at 550ºC (4 hr) and 1000ºC (2 hr), respectively (modified from Boyle, 2001; Heiri et al., 2001). The abundance of residual matter (lithics + biogenic silica) was calculated by subtracting %TOM from 100 % (%TC was not included because no carbonate was present). Magnetic susceptibility (MS) was measured on room temperature cores using a Geotek Multi-Sensor Core Logger at IUPUI and is reported in SI units $x10^{-5}$.

Age control

Age control for the Avery record was established by accelerator mass spectrometry (AMS) radiocarbon (^{14}C) analysis of 12 samples at the University of California, Irvine (UCI), Keck AMS Laboratory (Table 1). Charcoal and macroscopic terrestrial organic material > 63 µm was picked from a wet sieve after a brief disaggregation in a 7 % hydrogen peroxide solution. Samples were physically cleaned and chemically pretreated following acid-base-acid protocols

(Abbott and Stafford, 1996; Santos, 2011). Ages are reported as the median probability and 1σ error after calibration to calendar years before present (cal yr B.P.) using the online calibration program, Calib (Stuiver et al., 2018). Unless otherwise noted, dates in the text are referred to as being in the Common Era (CE) or before (BCE) with 1950 cal yr BP equal to 0 CE.

Grain size

Grain size samples were collected at ~4 cm intervals from the composite core (n = 233 samples). Approximately 1 g of wet sediment was dried for 24 hr at 60ºC, weighed, and then reacted with 30-35% H_2O_2 to remove organic matter (Gray et al., 2010). Diatoms were not observed in smear slides and LOI revealed no carbonate, so samples were not treated with NaOH or HCl. Grain size measurements were made using a Malvern Mastersizer 2000 with reported values being the average of three replicate measurements parsed into 49 particle size diameter bins between 0.1 and 2000 microns.

Organic carbon and total nitrogen elemental abundances and isotopic composition

The elemental abundances and isotopic composition of organic carbon (C_{org} & $\delta^{13}C_{org}$) and total nitrogen (N & $\delta^{15}N$) were determined for 150 samples (~6 cm resolution) at IUPUI (combustion with a Costech Analytical elemental analyzer coupled by continuous flow to a Thermo Delta V Plus isotope ratio mass spectrometer; IRMS) and Idaho State University (combustion with a Costech ECS 4010 elemental analyzer interfaced to a Thermo Delta V Advantage continuous flow IRMS). Approximately 10 mg of unacidified freeze-dried sample was weighed into tin capsules for isotopic analysis. The sample data are expressed in delta notation in units of per mil (‰) normalized to reference materials (USGS 40, RM 8704, RM

1577c). Analytical precision was better than ±0.2‰ for both $\delta^{13}C$ and $\delta^{15}N$ and < ± 0.5% of the sample value for %N and %C. The elemental standard acetanilide (C = 71.09%, and N = 10.36%) was used to correct elemental abundances based on the peak area response of the TCD detector.

Pollen

Pollen abundances were analyzed for 28 samples (1-cm^3 of sediment each) collected at variable depth intervals between 2 and 30 cm in order to focus on temporal areas of interest. Pollen was isolated from the sediment using standard techniques (Faegri & Iverson, 1989) and mounted in silicon oil. Each sample was examined under a light microscope at 400X and a minimum of 300 terrestrial pollen grains (including Cyperaceae) were identified and counted in each sample, to the finest taxonomic resolution possible (family-level or genus-level). The raw pollen counts were then converted to percentages based on the total terrestrial pollen sum.

X-ray fluorescence geochemistry

Geochemical analyses of the Avery sediments were made using a handheld Olympus Innov-X Delta Pro (DPO-6000-C) X-ray fluorescence analyzer. Titanium (Ti), zirconium (Zr), and lead (Pb) measured using two energy beams, each with a measurement time of 30 seconds. Beam one had an energy of 40 Kv and beam two had an energy of 10 Kv. Results were converted from counts per second to percent (%) abundance using the system's proprietary software and an Olympus calibration standard.

Results

Black Bottom geomorphic floodplain surfaces

To place Avery in the context of the evolving Black Bottom landscape, a map of distinct fluvial geomorphic surfaces was created by mapping cross-cutting relationships between ridges and swales visible on a 1 arc second digital elevation map (DEM; Fig. 2). Broadly, three terrace levels were identified (T1, T2, and T3). Although T3 and T2 were previously mapped as one landform (Alexander and Prior, 1971), we separated them because they represent distinct elevation surfaces in the DEM. The modern Ohio River floodplain, T1, is comprised of at least 12 discrete surfaces that represent different periods of floodplain construction. Avery is contained within unit 11a, which truncates units 8, 9a-c, 10a, and 10b, indicating that it is younger than these surfaces. The Kincaid Mounds archaeological site, in and around which were identified Baumer, Lewis, and Mississippian settlements, is located primarily on unit 8 and portions of 9a-c.

Avery Lake core stratigraphy

The 995 cm composite Avery core was visually divided into a basal section between 995 and 972 and an upper section above 972 cm. The basal section from 995 to 988 cm was composed of medium to coarse sand and gravel, which is consistent with the composition of modern and paleo Ohio River channel deposits (Alexander and Prior, 1971). From 988 to 972 cm, there were alternating layers of sandy silts and sand with abundant charcoal and macro organics. At 972 cm, there was an abrupt transition to massive, tan-to-buff colored, fine-grained sediments that persist to the top of the core (some banding occurs above 400 cm) and are consistent with lacustrine swale deposits on the Black Bottom (Alexander and Prior, 1971).

Chronology and sediment accumulation rates

All 12 AMS ^{14}C ages were in stratigraphic order, indicating continuous, undisturbed sediment accumulation. An age model for the Avery core was developed using linear interpolation between AMS ^{14}C ages (Fig. 3a). This method was chosen because output from the Bayesian age modeling software packages Bchron (Parnell et al., 2008) and Bacon (Blaauw and Christen, 2011) introduced uncertainties. For Bacon, the modeling software was unable to account for rapid changes in sedimentation rates, especially at and after 1100 CE. Although Bchron was better able to handle abrupt sedimentation rate transition better, the model introduced short lived, but abrupt changes in the age model that were not supported by the ^{14}C data.

A 1-cm-diameter stick located at 972.5 cm, just below the fluvial-lacustrine sediment transition, indicated that this transition occurred at 1130 BCE (3080 cal yr BP). Lacustrine sediment accumulation rates after this transition were calculated using both the linear age model and Bchron with the *acc_rate* function (Fig. 3b). The two methods show similar results. Sedimentation rates averaged 0.18 cm/yr from 1130 BCE to 50 CE. Between 50 and 1100 CE, sedimentation rates declined, reaching a minimum between 1000 and 1100 CE (0.01 cm/yr). Sedimentation rates abruptly increased to 0.50 cm/yr after 1100 CE, then decreased slightly to 0.40 cm/yr, averaging 0.46 cm/yr, until 1820 CE. The Bchron calculated accumulation rates differed slightly during this time, suggesting that sedimentation rates largely remained steady at 0.50 cm/yr. At 1820 CE, sedimentation rates abruptly increased again by 440% to 2.03 cm/yr and stayed at this level to the present. Increased sedimentation rates after 1820 CE in the Bchron model showed a slightly more gradual increase, but still reached 2.00 cm/yr during the most

recent part of the record. Importantly, the portion of the record above 1820 CE reflects four meters of accumulation, or approximately 40% of the composite Avery sediment archive, underscoring the unusually high sedimentation rates during the Eruo-American portion of the record.

Dry Bulk density, %TOM, and % Residual

Dry bulk density showed a decreasing trend from 1280 BCE to 110 CE, peaking at 1.66 g/cm^3 at 180 BCE and decreasing to 0.70 at 110 CE. From 110 to 1100 CE, BD varied about a mean of 0.72 g/cm^3. At 1100 CE, BD increased abruptly, averaging 0.96 until 1580 CE, after which point it decreased slightly to 0.82 g/cm^3 until 1790 CE. Dry BD then increased again from 1790 to 1940 CE, displaying two peaks at 1850 and 1920 CE, before it decreased from 1920 CE to the present (0.58 g/cm^3 in 2014 CE). Organic matter and %residual closely track the timing of BD trends, with %TOM mirroring BD and %residual being in phase. The only notable difference is that %TOM and %residual between 110 and 1100 CE respectively decreased and increased at 880 CE, 220 years before BD increased at 1100 CE.

Elemental abundances and isotopic composition of organic carbon and total nitrogen

The elemental ratio of organic carbon to total nitrogen (C/N) varied between 6 and 16.5 with the highest value occurring in the fluvial portion of the record (Fig. 4a). In the lacustrine portion of the record, C/N values increased from 1130 to 350 BCE with two peaks at 970 (10.7) and 540 BCE (13.6). At 340 BCE, C/N abruptly increased to 14.5 and remained high until 160 CE. Between 160 and 1100 CE, C/N remained relatively constant, averaging 11.3. C/N then decreased and remained low between 1100 and 1500 CE. Between 1500 and 1680 CE, C/N

increased, reaching a peak of 12.4. C/N then decreased to a low of 7.6 between 1730 and 1930 CE before generally increasing to the present.

Avery $\delta^{15}N$ ranged between 2.2 and 6.6 ‰. $\delta^{15}N$ was elevated between 1150 and 660 BCE (averaging 4.3 ‰) and then decreased sharply to 2.3 ‰ between 600 and 540 BCE. A broad increase in $\delta^{15}N$ subsequently occurred between 500 BCE and 160 CE (averaging 3.5 ‰). This period generally corresponds with the Baumer phase of occupation at Kincaid Mounds adjacent to Avery. After 160 CE, $\delta^{15}N$ remained low, averaging 2.8 ‰, until 920 CE. $\delta^{15}N$ increased to 3.7 ‰ at 1000 CE and then peaked between 1140 and 1460 CE, averaging 5.6 ‰ with a maximum of 6.5 ‰ between 1190 and 1210 CE. After 1460 CE, $\delta^{15}N$ decreased to an average of 3.6 ‰ until 1700 CE, after which point it increased again to the present, averaging 5.6 ‰ and peaking at 6.5 ‰ at 1880 CE. These latter two peaks, 1100 to 1460 CE and 1700 CE to the present, occured during known human occupations of the Black Bottom, with the former being associated with the Mississippian occupation and the latter Euro-American settlement. $\delta^{13}C$ was generally in-phase with $\delta^{15}N$ from ~500 BCE to the present ($r^2 = 0.63$, $p < 0.001$), showing peaks during the Baumer, Mississippian, and Euro-American phases. Before 500 BCE, $\delta^{13}C$ was low, averaging ~28.5 ‰ with two peaks approaching -27 ‰.

Grain size

The Avery core was dominated by silt (65.8 %) and clay (31.4 %) with minor amounts of sand (2.7 %; Fig 5). Variations in silt and clay were relatively minor within the lacustrine portion of the record, fluctuating by approximately 5 %. Sand concentration in contrast showed considerable variability. As would be expected, sand concentrations were very high during the fluvial portion of the Avery record with a peak of 81.9 % and an average of 50.9 % before 1130

BCE. Once the lacustrine environment was established, sand content immediately and substantially decreased, averaging just 1.0 %. Within the lacustrine portion of the record, however, there was still considerable variability. From 1130 to 60 BCE, sand concentration varied between 8.0 % and 0.0 % and generally decreased during this period. From 60 BCE to 1100 CE, sand concentration increased, peaking at 15.7 % between 920 and 1100 CE. At 1100 CE, sand concentration abruptly decreased and remained low until 1860 CE, averaging just 0.3 %. From 1860 CE to the present, sand concentration increased slightly, averaging 1.0 %.

Magnetic susceptibility and geochemistry

Magnetic susceptibility averaged 34.8 and showed considerable variability during the last 3000 years (Fig. 6a). Most noticeable are four prolonged peaks between 1300 and 1180 BCE, 370 and 70 BCE, 1100 and 1470 CE, and after 1730 CE with a particularly steep increase after 1830 CE that peaked in 1960 CE. These MS trends generally follow the geochemical trends represented by Ti, Zr and Pb, although with some differences (Fig. 6a-d). The main difference is that Ti and Zr were relatively high during the early part of the record, with Zr showing a peak between 800 and 290 BCE and subsequently decreasing to 250 CE; meanwhile, Ti generally decreased from the beginning of the record to 250 CE. After 250 CE, the MS, Ti, and Zr trends all closely tracked one another. Notably, MS tracked raw Pb concentrations as well as Pb trends normalized to Ti and Zr, except for the earliest peak in MS that was associated with fluvial deposits (Fig. 6e). Pb was normalized to the latter conservative elements because they are typically interpreted as reflecting input of terrestrial material from erosion. Normalizing Pb to Ti and Zr, therefore, removes trends associated with Pb derived from terrestrial sources. This assumption is supported by the similarities between the Zr and Ti trends and the BD and

%residual trends. Notably, the peaks in MS, Ti, and Pb between approximately 240-40 BCE, 1050-1500 CE, and after 1830 CE all correspond to periods of known occupation in the Black Bottom, i.e., the Baumer, Mississippian and Euro-American phases, respectively.

Pollen

The Avery pollen record demonstrates three distinct land use phases as seen in varying amounts of arboreal pollen (from trees) and non-arboreal pollen (from shrubs, grasses, and sedges; Fig. 7). Non-arboreal pollen was dominated by *Ambrosia* (ragweed; $r^2 = 0.81$ $p < 0.01$), with minor occurrences of Poaceae (grasses), Chenopodiaceae (goosefoot), *Iva* (marshelder), *Artemisia* (sagewort), and Cyperaceae (sedge). *Zea mays* (corn) pollen was also present, but only during the Mississippian period (1050 – 1400 CE) and after 1830 CE. Arboreal pollen was dominated by *Quercus* (oak), *Carya* (hickory), *Juglans* (walnut), *Ulmus* (elm), *Pinus* (pine), Cupressaceae (cedar), *Acer* (maple), and *Betula* (birch). The arboreal vs. non-arboreal pollen chart shows the strong antiphased behavior of the two pollen sets with each displaying three distinct highs and lows representing vegetation changes on the Black Bottom. From 1230 to 570 BCE, arboreal pollen varied between 77 and 96 %, while *Ambrosia* remained low (0 to 17 %). Arboreal pollen decreased (56 %) and *Ambrosia* pollen increased (35 %) between 340 BCE and 190 CE. This period notably coincided with the Baumer occupation at the adjacent site of Kincaid Mounds (Butler and Crow, 2013). From 360 to 1010 CE, arboreal pollen increased (88 %), while *Ambrosia* pollen decreased. Arboreal pollen subsequently decreased from 1100 to 1230 CE and remained low until sometime between 1370 and 1500 CE, while *Ambrosia* showed the opposite trend. This period of arboreal pollen decline and *Ambrosia* increase likewise corresponded to the documented Mississippian occupation of Kincaid Mounds from 1050 to

1400 CE (Butler et al., 2011). After 1500 CE, arboreal pollen increased and *Ambrosia* decreased once again following the end of the Mississippian occupation and respectively remained high (90 %) and low (1.4 %) until 1850 CE when Euro-American settlers cleared the bottom for agriculture. With the exception of the transition to the Mississippian occupation, which is covered by a high-resolution sample interval, the precise timing of other transitions will need to be refined by analyzing more samples. Nonetheless, the pollen data capture a detailed record of vegetation changes on the Black Bottom.

Discussion

Temporal evolution of the Black Bottom

Geomorphic research investigating the Holocene development of the Black Bottom floodplain was first conducted in the late 1960s and early 1970's (Alexander and Prior, 1968, 1971; Alexander and Nunnally, 1972). This work combined sedimentological observations and a series of radiocarbon dates on organic matter collected from bucket type auger borings of the floodplain, ridges, and Avery swale, and additional dates on tree stumps eroding out of the modern Ohio River banks (Fig. 2). One date on organic matter collected at 120 cm depth from a ridge just south of the Avery Swale (GX 1473) on surface 14 dated to 5750 cal yr BP (Fig. 2). Another date from a tree stump at Kincaid Landing (GX 340) on the southern tip of the Black Bottom returned an age of 1250 cal yr BP (Fig. 1). Based on these data, Alexander and Nunnally (1972) concluded that the Black Bottom floodplain had formed and the Ohio River had assumed its current planform by the middle Holocene, thereafter remaining in dynamic equilibrium.

The new Avery chronology contradicts these results indicating that the land surface in which Avery Lake is contained (surface 11a) formed no earlier than 3080 cal yr BP, ~3000 years

later than initially concluded (Fig. 2 & 3; Table 1). The implication that the Ohio River did not establish its modern plan form during the middle Holocene suggests a river more mobile than previously concluded as it has not maintained its current position since the middle Holocene vis-à-vis dynamic equilibrium. Future work therefore needs to be directed toward understanding how dynamic the lower Ohio River has been and whether or not the formation of the Black Bottom and other floodplains was continuous or sporadic and the role that long-term Holocene climate and land-use played in determining its dynamics.

Late Holocene Black Bottom sedimentation rates and land-use

Sedimentation across the Black Bottom is predominantly controlled by annual floods that exceed 12.2 m above the modern Ohio River water level (Alexander and Nunnally, 1971). Variations in the rate of sediment accumulation are, therefore, closely linked to the occurrence of floods of sufficient magnitude to inundate the Black Bottom, providing a means by which to investigate the relationship between climate and fluvial dynamics.

Using ^{14}C-dated vertical sequences from ridges (n = 3) and the Avery swale (n = 6), Alexander and Nunnally (1971) estimated sediment accumulation rates of 0.27 to 6 mm/yr on ridges and 1.9 mm/yr in the swales. It was additionally suggested that sedimentation rates had increased during the last 1500 years, possibly in response to land-use changes associated with agriculture. The Avery chronology contrasts with these results, indicating that the upper four meters of the Avery sediment column represents alluvium deposited over the last ~200 years. It is possible that the different coring locations may account for these chronological differences; however, two of the six dates of the Alexander and Nunnally (1971) chronology were reversed and all had large associated errors, suggesting that the chronology does not accurately reflect the

temporal depositional history of the Black Bottom. Here we focus on the new Avery chronology to investigate late Holocene sediment accumulation rates and their relationship with anthropogenic and climatic drivers.

Avery's sedimentation rates show considerable variability during the last ~3100 years that suggest possible changes in Ohio River flooding (Fig. 8a). First, however, we investigate signatures of anthropogenic activities on the Black Bottom that are preserved in the Avery sediment archive in order to evaluate if human activities may have influenced Avery sedimentation rates in addition to flooding.

Anthropogenic impacts on the Black Bottom that began ~200 years ago are still visible today; the floodplain is largely deforested and supports typical Eastern Corn Belt row crop agriculture, primarily corn and soybeans. This is reflected in the Avery pollen record, which shows the presence of *Zea mays* pollen (Fig. 8e). Sediments from the last 200 years also contain high percentages of *Ambrosia* pollen and reduced forest pollen, which is consistent with a deforested state of the Black Bottom (Fig. 8e & f). This trend was not unique to the Black Bottom, however, as over 90% of the eastern United States was deforested in the 1800s and early 1900s in order to make room for agriculture, procure timber for construction purposes, and expand urban footprints (Greeley, 1925).

Additional evidence for modern anthropogenic impacts on floodplain sedimentation rates is provided by the highest sedimentation rates (2.0 cm/yr) and magnetic susceptibility values occurring in the most recent 200 years of the Avery record (Fig. 8a). This is consistent with findings that deforested natural landscapes in the Midwest (forest or prairie) were significantly eroded and that their sediment yield translated into large increases in floodplain

accumulation rates (Knox, 1987; Miller et al., 1993; Fitzpatrick et al., 1999; Fitzpatrick and Knox, 2000; Knox, 2006).

Modern human influences are also observable in other indicators like $\delta^{15}N$, Pb/Ti, and $\delta^{13}C$. Increases in $\delta^{15}N$ during the last 200 years mostly likely reflects increasing Euro-American population densities in the Ohio River watershed since the late 1700s (Cabana and Rasmussen, 1996) and the use of organic fertilizers (Bateman and Kelly, 2007). The slight decrease in $\delta^{15}N$ over the last 60 years may be due to the increasing use of synthetic fertilizers, which have a $\delta^{15}N$ value close to 0 ‰ (Bateman and Kelly, 2007) and/or increased cultivation of symbiotic N-fixers, like soybeans, that also have $\delta^{15}N$ value close to 0 ‰ . High $\delta^{13}C$ during the last 200 years may likewise reflect greater in-lake productivity as a result of increased nutrient supply from population increases and pervasive agriculture. This is supported in part by reduced C/N during the Euro-American period, suggesting greater aquatic productivity. The slight increase in C/N during the last 50 years could reflect a shallowing of the lake and/or increased local erosion. Synchronous increases in Pb pollution during the Euro-American period likely reflect the widespread combustion of coal in the 1800s and later the use of leaded gasoline, in addition to other industrial activities (Graney et al., 1995).

Widespread land-use on Black Bottom was not limited to the last 200 years. Extensive archaeological research demonstrates a long history of Native American settlement on the Black Bottom prior to the Euro-American period. The Kincaid Mounds site, which is directly adjacent to Avery, was the focal point for the best documented of these occupations, which include the Mississippian (1150-1400 CE), Lewis (650-900 CE), and Baumer (300 BCE to 300 CE) phases (Figs. 2 & 8; Butler and Welch, 2006; Brennan, 2014; Butler, 2014; Muller, 2016). Landscape impacts associated with Mississippian and Baumer occupations are especially apparent in

decreases in forest pollen and increases in *Ambrosia* pollen, the magnitude of which suggest that local land clearance during these phases was analogous with that which occurred during the last 200 years. The Mississippian occupation has typically been viewed as being more extensive than the Baumer or Lewis phase occupations, in part because the construction of monumental earthworks (i.e., the Kincaid Mounds) that occurred during this time and the intensive maize agriculture that was practiced. Increases in $\delta^{15}N$ that are equivalent in magnitude to the modern $\delta^{15}N$ peak support this idea, suggesting that Kincaid Mounds supported a dense population, possibly reaching to between 60 to 80 people/km^2 (Cabana and Rasmussen, 1996). It is notable, however, that the magnitude and duration of land clearance during the Baumer phase appears to have been greater than the Mississippian phase, given the more prolonged high abundance of *Ambrosia*, and higher abundances of Chenopoadiceae (both of which respond positively to disturbance), and decreased arboreal pollen abundances, despite lower $\delta^{15}N$. Low $\delta^{15}N$ is consistent with reduced Baumer populations during this phase, but indicates they had a greater proportional impact on the landscape. Like during the Euro-American period, $\delta^{13}C$ increased during the Mississippian and, to a lesser extent, Baumer occupations, suggesting that increased nutrient supply may have stimulated in-lake productivity. Although low C/N and high $\delta^{15}N$ values support this interpretation for the Mississippian period, high C/N and low $\delta^{15}N$ values during the Baumer phase suggest a different relationship. One possibility is that the modestly increased in-lake productivity was driven by nutrients supplied by extensive land clearance when human populations were small.

Notably, Pb pollution and magnetic susceptibility both show similar increases during the Baumer and Mississippian phases that suggest consistent associations between these indicators and human land-use. Although pre-Euro-American sources of Pb pollution are not

well known, it is possible that extensive land clearance using fire and/or lead (galena) working contributed to Pb pollution (Walthall, 1981; Larson and Koenig, 1994; Graney et al., 1995).

Avery Lake sedimentation rates appear not to have been affected by the pre-Columbian occupation periods between 1130 BCE and 1830 CE identified in the proxy data. For instance, sedimentation rates fluctuated little during the Baumer phase between 1130 BCE and 300 CE, mostly varying about a mean of 0.18 cm/yr, despite pollen data indicating a cleared landscape (Fig. 8). Although sedimentation rates increased sharply at the start of the Mississippian occupation (1100 CE) to 0.50 cm/yr, these rates were maintained for ~350 years after the Mississippians abandoned Kincaid Mounds and the Black Bottom (between 1400-1450 CE) (Cobb and Butler, 2002) and the forest had regenerated (< 50 years after abandonment). These results suggest that sedimentation rates on the Black Bottom between 1130 BCE and 1830 CE were not significantly impacted by pre-Columbian Native American land-use and that other factors, such as changes in flooding regimes, were responsible. This conclusion is further supported by recent work on the White River, IN, a moderately sized tributary of the Ohio River (watershed = 14,880 km^2), which shows floodplain accretion as a result of overbank flooding occurred when sedimentation rates were high at Avery (Fig. 9e) (Herrmann and Monaghan, 2018). Conversely, periods when overbank flooding was absent or minimal on the White River, sedimentation rates were low at Avery. This suggests that overbank flooding on the lower Ohio River and White Rivers were in phase, supporting a common driver of this regionally coherent signal.

Climate-flood relationships before 1830 CE

Relationships between flooding and climate on the Black Bottom were investigated by comparing the Avery sedimentation rates, sand concentrations, and %residual (i.e., %lithics) data with recently published climate reconstructions from Martin Lake, IN (Fig. 9; Bird et al., 2017b). Percent sand and residual trends at Avery closely track sedimentation rates, suggesting that these proxies were not significantly affected by land-use changes, but instead reflect climate-flood dynamics. Sand concentrations, for example, are generally less than 1% except for between ~500 and 1100 CE when they increase to nearly 20%. The lowest sedimentation rates of the last 3,100 years occurred at this time, suggesting that the increase in sand reflect low lake levels (Håkanson, 1982; Bird et al., 2017a; Bird et al., 2018). Residual abundances (interpreted as reflecting the lithic fraction) showed generally opposite trends, with relatively high values before 300 CE and after 1100 CE and low values in between. The one exception was an increase in %residual between 900 and 1100 CE, which corresponded to the sand peak. Increased lithics during this suspected dry period is consistent with low lake levels because receding waters would have winnowed lithics and sand together toward the center of the lake. Residual abundances were otherwise in phase with sedimentation rates between 1130 BCE and 1830 CE, supporting a tripartite division of late Holocene climate.

A more nuanced picture of Midwestern hydroclimatic controls on flooding and sedimentation during the past 3000 years emerges when comparing the three Avery proxies with records of climate variability from nearby Martin Lake, IN (Fig. 9). The Martin %lithics record reflects variations in the amount of material washed into the lake during warm-season rainstorm events. The Martin authigenic calcite oxygen isotope record ($\delta^{18}O$) in turn reflects the seasonality of precipitation and the source from which it was derived. Variations in the seasonality and source of Midwest precipitation captured by the Martin Lake record were

attributed to variations in atmospheric circulation that resemble the Pacific North American Mode (PNA), the primary driver of modern US climate variability (Wallace and Gutzler, 1981; Coleman and Rogers, 2003; Bird et al., 2017b). Negative (-) PNA modes are characterized by west to east zonal flow that strengthens clockwise atmospheric circulation over the Gulf of Mexico, which increases moisture delivery (typically rain) into the Midwest. Positive (+) PNA phases are conversely associated with strong ridge (over the western US) and trough (over the Midwest) atmospheric circulation that increases delivery of moisture (typically snow) from the Pacific Northwest and Arctic. Together, the Martin Lake data indicate that when Northern Hemisphere temperatures were warm (Mann et al., 2009), warm-season precipitation from the Gulf of Mexico dominated and warm-season rainstorm events were more frequent (-PNA). Conversely, when Northern Hemisphere temperatures were cool, cold-season precipitation originating from Pacific and Arctic sources dominated and warm-season rainstorm events were considerably less frequent, resulting in warm-season drought (+PNA; Fig. 9f-h).

Comparing the Martin Lake records with the Avery data prior to 1830 CE shows that when climate was dominated by cold-season precipitation from the Pacific and Arctic (+PNA conditions), sedimentation rates and clastic deposition were high. Indeed, the strongest cold-season anomaly, which occurred between 1150-1830 CE, and includes the Little Ice Age (1250-1830 CE), corresponded to the highest sedimentation rates prior to the Euro-American period. Conversely, when warm-season precipitation dominated between 350 and 1150 CE (-PNA conditions), Avery sedimentation rates and lithic abundances were at their lowest point and sand abundances were at their highest for the ~3000-year interval prior to 1830 CE. This suggests that lower Ohio River flooding during the late Holocene was largely controlled by precipitation seasonality related to PNA-like atmospheric circulation, whereby floods of sufficient magnitude

to inundate Avery were more frequent during times when winter precipitation predominated under +PNA-like mean state conditions.

Importantly, PNA variability is closely linked to the Pacific atmosphere-ocean system such that positive and negative PNA modes are respectively associated with decadal modes atmosphere-ocean variability (the Pacific Decadal Oscillation; PDO) that resemble El Nino and La Nina conditions (Yu and Zwiers, 2007). Comparison of the Martin Lake data with reconstructed North Pacific sea surface temperatures (SST) spanning the last 1500 years shows that Midwest PNA-like atmospheric circulation closely tracks SST variability associated with the PDO (Fig. 9i) (Mann et al., 2009). When compared with the Avery flood reconstruction, it is seen that minimum flooding occurred under largely -PDO and -PNA mean state conditions between 500 and 1150 CE. The abrupt increases in flooding at Avery notably occurred during a marked shift to +PDO and +PNA conditions after 1150 CE. These relationships strongly suggest that lower Ohio River flooding prior to anthropogenic landscape modifications in the 1800s was tightly linked with Pacific atmosphere ocean variability through the PNA. This finding is consistent recent work that shows lower Mississippi River flood events during the last 500 years were closely associated with El Nino-like conditions in the Pacific (Munoz et al., 2018).

The regional impact of these climatic forcings on fluvial systems is additionally apparent in the opposing sedimentological responses demonstrated by Avery and Martin to the same climatic forcing. Annual floods in large (> 1000 km^2) temperate watersheds, like the Ohio River, are typically associated with spring snowmelt because the simultaneous melting of snow across these watersheds produces a cumulative discharge in trunk streams that is sufficient to result in large annual floods (Knox, 1988, 2000; Knox and Daniels, 2002). Snowmelt in small, low-gradient watersheds, like Martin Lake (the headwaters of the East Fork Elk Heart River, IN),

however, is insufficient to create the volume of high-energy surface flow necessary to cause floods and transport large quantities of sediment. Instead, flooding and erosion in small watersheds is largely controlled by the occurrence of intense convective warm-season rainstorms. However, such warm-season precipitation events are typically not of sufficient spatial extent or duration to produce the runoff necessary to create large floods in trunk streams. In addition, infiltration and evapotranspiration rates during the warm-season are high, which reduces basin-scale runoff and results in smaller discharges in large trunk streams.

Euro-American impacts on flooding (post 1830 CE)

Our results support the idea that seasonal changes in precipitation related to PNA and PDO variability were leading drivers of flooding in both large (e.g., the lower Ohio River) and small (e.g., Martin Lake) Midwest watersheds in ways that are consistent with the modern understanding of scale-dependent watershed responses to climate discussed above. However, this relationship appears to have broken down after 1830 CE. After 1830 CE, sedimentation rates at Avery increased almost five-fold, sand concentrations remained near 1 %, and lithic deposition remained high, despite a shift to a warm-season dominated precipitation regime characterized by -PNA and -PDO mean states (Fig. 9). The timing of this change in response pattern coincides exactly with the widespread deforestation of much of the eastern United States (Greeley, 1925), and suggests that the former may be a response to the latter.

Several lines of evidence indicate that land-use changes after 1830 CE (such as deforestation, landscape conversion for agriculture, and urbanization) in the Ohio River watershed changed runoff dynamics through altered infiltration rates. Primary accounts also document that in 1830 the Corps of Engineers began removing log jams and dredging channels

in the Ohio River (Sanders, 1991). In this scenario, post-1830 land-use reduced infiltration, which allowed increased warm-season precipitation runoff and ultimately permitted sizeable floods to be generated in large trunk streams, like the Ohio River. This idea is consistent with increased landscape erosion and runoff, and subsequently increased stream discharge and sediment yield, at the time that natural landscapes (forest or prairie) were converted to agricultural lands in the upper Mississippi River Valley (Fitzpatrick and Knox, 2000; Knox, 2006; Munoz et al., 2018). Additionally, the Martin Lake $\delta^{18}O$ record suggests that the shift to warm-season precipitation (-PNA conditions) after 1830 CE was more pronounced than at any other time in at least the last 2000 years. Whereas previous periods predominated by warm-season precipitation had some cold-season anomalies (e.g., 350 to 1250 CE), no persistent cold-season precipitation anomalies are apparent during the last 200 years (Fig. 9f). This suggests that the recent shift to warm-season precipitation is unique within the context of the late Holocene and that there may also be more frequent atmospheric river events during this time. Nonetheless, we argue that these climate changes alone are not sufficient to account for recent flooding trends. We contend that land-use changes that dramatically increased runoff have fundamentally changed the hydrology of the Ohio River watershed, such that it became highly sensitive to warm-season precipitation and atmospheric river events in particular. Were pre-Euro-American ecosystems intact, current warm-season dominated climatic conditions would likely not result in the degree of landscape erosion and flooding that is observed today.

Conclusions

The Avery chronology and data indicates that portions of the Black Bottom floodplain formed during the late Holocene (after 3080 yr BP), and not in the middle Holocene (~5650 cal

yr BP) as previously estimated, which calls into question the idea that portions of the lower Ohio River were relatively stability during the Holocene, maintaining their current plan form for thousands of years via dynamic equilibrium. Instead, we suggest that the lower Ohio River is more dynamic than previously concluded.

Our results suggest that although the Black Bottom has a long history of late Holocene human occupations, pre-Euro-American cultures did not contribute significantly to landscape erosion. Instead, changes in sedimentation rates before 1830 CE are attributed to variations in average flood occurrences. Comparison of the Avery flood record with high-resolution Midwest climate reconstructions indicate that flooding occurrence on the lower Ohio River before 1830 CE was closely associated with the predominance of cold-season precipitation from Pacific and Arctic sources during +PNA and +PDO mean states. Conversely, flooding was reduced when warm-season precipitation from the Gulf of Mexico predominated during -PNA and -PDO mean states. We suggest that largely synchronous seasonal snowmelt across the Ohio River watershed during cold-season-dominated events increased regional runoff, which in turn increased the magnitude and frequency of seasonal floods. In contrast, less regionally coherent warm-season precipitation combined with increased infiltration and evapotranspiration, reduced the magnitudes and frequencies of floods on the lower Ohio River during times when warm season precipitation from the Gulf of Mexico predominated.

A shift in the last 200 years, however, to regular large magnitude floods and very high sedimentation rates (2.03 cm/yr) despite the predominance of warm-season precipitation represents a fundamental shift in the Ohio River climate-flood dynamic. We suggest that watershed-scale hydrologic adjustments to land-use changes (i.e., reduced infiltration and increased runoff in response to extensive deforestation during landscape conversion for

agriculture and urbanization), and extensive modification of the river system itself, have increased the impact of warm-season precipitation events. Warm-season precipitation events, including atmospheric river events, may also be more frequent during the current climate state, increasing flooding and erosion on landscapes that are less resilient to extreme rainfall because of extensive anthropogenic modification. Based on our analysis of ~3,000 years of pre-Euro-American climate-flooding relationships, the current climatic regime, including the increase in annual average precipitation and more frequent extreme precipitation events, would not have produced the increase in flooding, landscape erosion, and sediment yields presently observed across the midcontinental US if floodplain and upland landscapes were intact.

Acknowledgements

Partial support for this research was provided by a National Science Foundation Research Experiences for Undergraduates grant awarded through the Office of Multidisciplinary Activities within Social, Behavioral & Economic Sciences (NSF SMA 1262530), Indiana University's Collaborative Research Grant program, and IUPUI's Multidisciplinary Undergraduate Research Initiative (MURI). We also acknowledge the contributions of student researchers that participated in the MURI (Olabode Dawodu, Kylie Grout, Emilee Jennings, Tori Kennedy, LeAnne Lautenhiser, Justin Lazaro) and NSF REU programs (Haley Burkhardt, Eliza Kane, Tara Miller, Ashley Packard, Aaron Stump, Gloria Thomas, Ryan Walsh, Kristen Twidt, Savanna Johnson).

Figure Captions

Figure 1 a) Regional map of the Ohio River (blue line) and its watershed (gray shading) showing the location of the study area (red rectangle). b) Shaded digital elevation map (color scale in

meters) of the study area showing the Black Bottom point bar floodplain and terraces 1 (T1; red dashed line), 2 (T2; white dashed line), and 3 where T3 is the active modern floodplain. The locations of radiocarbon samples from Alexander and Prior (1971) are shown with white boxes. Green circles mark the locations of the Avery Lake cores discussed in this study. The dashed black line indicates the location of the Kincaid Mounds archaeological site adjacent to Avery Lake. c) Expanded view of Avery Lake and the adjacent Kincaid Mounds archaeological site with the positions of structures, mounds, and palisades after Butler (2014). The location of cores used in this study (A-14 and B-14) are shown with green circles.

Figure 2 Digital elevation map of the Black Bottom showing the different geomorphic surfaces of the point bar as determined by mapping cross-cutting relationships between ridges and swales. Increasing number indicate relatively younger geomorphic surfaces, such that surface 1 on T1 is the oldest geomorphic surface and surface 14 at the tip of the point bar is the youngest, or most recently formed. Surfaces that could not be relatively dated with respect to one another have the same surface age number, but different sub-letters, e.g., 9a and 9b.

Figure 3 a) Avery Lake radiocarbon ages (black circles) plotted versus depth (y-axis). The error, both for depth and age, of the sample is less than the size of the symbol. b) Sediment accumulation rates at Avery Lake as determined by linear interpolation between radiocarbon dates (black line) and using Bchron (red line). Sedimentological data from the Avery Lake core, including c) dry bulk density, d) % organic matter, and e) percent residual (i.e., lithic abundance). The gray vertical box indicates the portion of the record where sediment was of fluvial origin as opposed to lacustrine-fluvial.

Figure 4 Geochemical and isotopic results of organic matter from Avery Lake for a) C/N, b) $\delta^{15}N$, and c) $\delta^{13}C$. The light gray vertical box indicates the portion of the record deposited when Avery Lake was still a paleo-channel of the Ohio River. Dark gray vertical boxes indicate known human occupations of the Kincaid Mounds site later in the record, including the Baumer, Lewis, Mississippian, and Euro-American periods.

Figure 5 a) Shaded histogram of the grain size results from Avery Lake. The shading indicates the abundance of grain sizes within the corresponding grain size diameter range. Horizontal solid lines denote the separations between clay, silt and sand according to the Wentworth grain size scale. Individual time series for b) %sand, c) %silt, and d) %clay are also shown. The gray vertical box indicates the portion of the record deposited when Avery Lake was still a paleo-channel of the Ohio River. Dark gray vertical boxes indicate known human occupations of the Kincaid Mounds site later in the record, including the Baumer, Lewis, Mississippian, and Euro-American periods.

Figure 6 a) Magnetic susceptibility results for Avery Lake. XRF geochemistry results from Avery Lake for b) % zirconium, c) % titanium, d) lead in parts per million, e) and the ratio of Pb/Zr (black Line) and Pb/Ti (red line) are also shown. The light gray vertical box indicates the portion of the record deposited when Avery Lake was still a paleo-channel of the Ohio River. Dark gray vertical boxes indicate known human occupations of the Kincaid Mounds site during the Baumer, Lewis, Mississippian, and Euro-American periods.

Figure 7 Time series for selected major components of the pollen assemblage (in %) preserved in the Avery Lake record, including arboreal a) *Carya* (Hicory), b) *Ulmus* (Elm), c) *Juglans* (Walnut) and non-arboreal d) *Ambrosia* (Ragweed), e) Chenopodiaceae (Goosefoot), f) Poaceae (grasses), and g) *Zea mays* (corn). Total h) arboreal and i) non-arboreal pollen abundance timeseries are also shown. Gray shading indicates periods of occupation on the Black Bottom as in Fig. 6.

Figure 8 Comparison of Avery Lake a) sedimentation rates, b) $\delta^{15}N$, c) Pb/Ti, and d) magnetic susceptibility with e) non-arboreal pollen from *Ambrosia* and *Zeya Mays* and f) arboreal (tree) pollen. Gray vertical boxes are as defined in Figure 7.

Figure 9 a) Climate-flooding regime relationships as indicated by comparison of Avery Lake a) sedimentation rates, c) %sand, and d) %residual with the e) White River, IN, vertical accretion record and Martin Lake, IN, e) %lithics and f) precipitation $\delta^{18}O$ (Herrmann and Monaghan, 2018). Also shown are h) Northern Hemisphere temperatures and i) North Pacific SST anomalies from Mann et al. (2009). Light gray shading indicates periods of increased overbank flooding and sediment accumulation along the lower Ohio River as identified at Avery Lake. Dark gray shading indicates periods of reduced overbank flooding and sediment accumulation along the lower Ohio River according to the Avery record.

References

Abbott MB and Stafford TW. (1996) Radiocarbon geochemistry of modern and ancient Arctic lake systems, Baffin Island, Canada. *Quaternary Research* 45: 300-311.

Alexander CS and Nunnally NR. (1972) Channel stability on the lower Ohio River. *Annals of the Association of American Geographers* 62: 411-417.

Alexander CS and Prior JC. (1968) The origin and function of the Cache Valley, southern Illinois. *The Quaternary of Illinois: Urbana, University of Illinois College of Agriculture Special Publication* 14: 19-26.

Alexander CS and Prior JC. (1971) Holocene sedimentation rates in overbank deposits in the Black Bottom of the lower Ohio River, southern Illinois. *American Journal of Science* 270: 361-372.

Andresen J, Hilberg S, Kunkel K, et al. (2012) Historical climate and climate trends in the Midwestern USA. *US National Climate Assessment Midwest Technical Input Report*: 1-18.

Bartlein PJ, Webb T and Fleri E. (1984) Holocene climatic change in the northern Midwest: pollen-derived estimates. *Quaternary Research* 22: 361-374.

Bateman AS and Kelly SD. (2007) Fertilizer nitrogen isotope signatures. *Isotopes in Environmental and Health Studies* 43: 237-247.

Bird BW, Lei Y, Perello M, et al. (2017a) Late Holocene Indian summer monsoon variability revealed from a 3,300-year-long lake sediment record from Nir'pa Co, southeastern Tibet. *The Holocene* 27: 541-552.

Bird BW, Rudloff O, Escobar J, et al. (2018) Paleoclimate support for a persistent dry island effect in the Colombian Andes during the last 4700 years. *The Holocene* 28: 217-228.

Bird BW, Wilson JJ, Gilhooly III WP, et al. (2017b) Midcontinental Native American population dynamics and late Holocene hydroclimate extremes. *Scientific Reports* 7: 41628.

Blaauw M and Christen JA. (2011) Flexible paleoclimate age-depth models using an autoregressive gamma process. *Bayesian Analysis* 6: 457-474.

Booth RK, Notaro M, Jackson ST, et al. (2006) Widespread drought episodes in the western Great Lakes region during the past 2000 years: geographic extent and potential mechanisms. *Earth and Planetary Science Letters* 242: 415-427.

Boyle JF. (2001) Inorganic geochemical methods in paleolimnolgy. In: Smol WMLJP (ed) *Tracking Environmental Change Using Lake Sediments.* Dordrecht, The Netherlands: Kluwer Academic Publishers, 83-141.

Brennan TK. (2014) *Mississippian community-making through everyday items at Kincaid Mounds*: Southern Illinois University at Carbondale.

Bridge JS. (2009) *Rivers and floodplains: forms, processes, and sedimentary record*: John Wiley & Sons.

Butler BM. (2008) Land between the Rivers: The Archaic Period in Southernmost Illinois. *Archaic Societies: Diversity and Complexity Across the Midcontinent, edited by T. Emerson, D. McElrath, and A. Fortier*: 607-634.

Butler BM, Clay RB, Hargrave ML, et al. (2011) A new look at Kincaid: magnetic survey of a large Mississippian town. *Southeastern Archaeology* 30: 20-37.

Butler BM and Crow R. (2013) Archaic Period Occupation at Kincaid Mounds. *Illinois Archaeology* 25: 75-109.

Butler BM, Paul D. Welch, Tamira K. Brennan and Corin C. O. Pursell. (2014) Kincaid in the New Century: Recent Investigations of A Prehistoric Illinois Metropolis. In: Wilson JJ and Krus AM (eds) *A View from Upstream: Late Pre-Columbian Research in the Ohio Valley.* Gainesville: University of Florida Press.

Butler BM and Welch PD. (2006) Mounds lost and found: New research at the Kincaid site. *Illinois Archaeology* 17: 138-153.

Cabana G and Rasmussen JB. (1996) Comparison of aquatic food chains using nitrogen isotopes. *Proceedings of the National Academy of Sciences* 93: 10844-10847.
Cobb CR and Butler BM. (2002) The vacant quarter revisited: late Mississippian abandonment of the Lower Ohio Valley. *American Antiquity*: 625-641.
Coleman JS and Rogers JC. (2003) Ohio River Valley winter moisture conditions associated with the Pacific-North American teleconnection pattern. *Journal of Climate* 16: 969-981.
Counts RC, Murari MK, Owen LA, et al. (2015) Late Quaternary chronostratigraphic framework of terraces and alluvium along the lower Ohio River, southwestern Indiana and western Kentucky, USA. *Quaternary Science Reviews* 110: 72-91.
Denniston RF, González LA, Asmerom Y, et al. (1999) Evidence for increased cool season moisture during the middle Holocene. *Geology* 27: 815-818.
Dirmeyer PA and Kinter III JL. (2010) Floods over the US Midwest: A regional water cycle perspective. *Journal of Hydrometeorology* 11: 1172-1181.
Fitzpatrick FA and Knox JC. (2000) Spatial and temporal sensitivity of hydrogeomorphic response and recovery to deforestation, agriculture, and floods. *Physical Geography* 21: 89-108.
Fitzpatrick FA, Knox JC and Whitman HE. (1999) Effects of historical land-cover changes on flooding and sedimentation, North Fish Creek, Wisconsin. US Geological Survey.
Graney J, Halliday A, Keeler G, et al. (1995) Isotopic record of lead pollution in lake sediments from the northeastern United States. *Geochimica et Cosmochimica Acta* 59: 1715-1728.
Gray AB, Pasternack GB and Watson EB. (2010) Hydrogen peroxide treatment effects on the particle size distribution of alluvial and marsh sediments. *The Holocene* 20: 293-301.
Greeley WB. (1925) The relation of geography to timber supply. *Economic Geography* 1: 1-14.
Håkanson L. (1982) Lake bottom dynamics and morphometry: The dynamic ratio. *Water Resources Research* 18: 1444-1450.
Heiri O, Lotter AF and Lemcke G. (2001) Loss on ignition as a method for estimating organic and carbonate content in sediments: reproducibility and comparability of results. *Journal of Paleolimnology* 25: 101-110.
Herrmann EW and Monaghan GW. (2018) Post-glacial drainage basin evolution in the midcontinent, North America: Implications for prehistoric human settlement patterns. *Quaternary International*
Knox JC. (1983) Responses of river systems to Holocene climates. In: Wright H (ed) *Late quaternary environments of the United States.* Minneapolis, USA: University of Minnesota Press, 26-41.
Knox JC. (1984) Fluvial responses to small scale climate changes. *Developments and applications of geomorphology.* Springer, 318-342.
Knox JC. (1985) Responses of floods to Holocene climatic change in the Upper Mississippi Valley. *Quaternary Research* 23: 287-300.
Knox JC. (1987) Historical valley floor sedimentation in the Upper Mississippi Valley. *Annals of the Association of American Geographers* 77: 224-244.
Knox JC. (1988) Climatic influence on upper Mississippi valley floods. *Flood Geomorphology. John Wiley & Sons New York. 1988. p 279-300. 9 fig, 6 tab, 43 ref. National Science Foundation Grant EAR-8306171.*
Knox JC. (2000) Sensitivity of modern and Holocene floods to climate change. *Quaternary Science Reviews* 19: 439-457.

Knox JC. (2006) Floodplain sedimentation in the Upper Mississippi Valley: Natural versus human accelerated. *Geomorphology* 79: 286-310.
Knox JC and Daniels JM. (2002) Watershed scale and the stratigraphic record of large floods. *Ancient Floods, Modern Hazards*: 237-255.
Laird KR, Fritz SC and Cumming BF. (1998) A diatom-based reconstruction of drought intensity, duration, and frequency from Moon Lake, North Dakota: a sub-decadal record of the last 2300 years. *Journal of Paleolimnology* 19: 161-179.
Larson TV and Koenig JQ. (1994) Wood smoke: emissions and noncancer respiratory effects. *Annual review of public health* 15: 133-156.
Lavers DA and Villarini G. (2013) Atmospheric rivers and flooding over the central United States. *Journal of Climate* 26: 7829-7836.
Liu Z, Yoshimura K, Bowen GJ, et al. (2014a) Paired oxygen isotope records reveal modern North American atmospheric dynamics during the Holocene. *Nature communications* 5.
Liu Z, Yoshmura K, Bowen GJ, et al. (2014b) Pacific–North American teleconnection controls on precipitation isotopes ($\delta^{18}O$) across the contiguous United States and adjacent regions: A GCM-based analysis. *Journal of Climate* 27: 1046-1061.
MacNeish RS. (1948) The pre-pottery Faulkner site of southern Illinois. *American Antiquity* 13: 232-243.
Mallakpour I and Villarini G. (2015) The changing nature of flooding across the central United States. *Nature Climate Change* 5: 250-254.
Mann ME, Zhang Z, Rutherford S, et al. (2009) Global signatures and dynamical origins of the Little Ice Age and Medieval Climate Anomaly. *Science* 326: 1256-1260.
Miller SO, Ritter DF, Kochel RC, et al. (1993) Fluvial responses to land-use changes and climatic variations within the Drury Creek watershed, southern Illinois. *Geomorphology* 6: 309-329.
Monaghan GW and Lovis WA. (2005) *Modeling archaeological site burial in southern Michigan: a geoarchaeological synthesis*: MSU Press.
Muller J. (2016) *Archaeology of the lower Ohio river valley*: Routledge.
Munoz SE, Giosan L, Therrell MD, et al. (2018) Climatic control of Mississippi River flood hazard amplified by river engineering. *Nature* 556: 95.
Parnell AC, Haslett J, Allen JR, et al. (2008) A flexible approach to assessing synchroneity of past events using Bayesian reconstructions of sedimentation history. *Quaternary Science Reviews* 27: 1872-1885.
Pryor SC, Scavia D, Downer C, et al. (2014) Chapter 18: Midwest. *Climate Change Impacts in the United States: The Third National Climate Assessment. US Global Change Research Program, Washington, DC* http://nca2014.globalchange.gov/report/regions/midwest.
Robinson BA. (2013) *Regional bankfull-channel dimensions of non-urban wadeable streams in Indiana*: US Department of the Interior, US Geological Survey.
Sanders S. (1991) Always a River: The Ohio River and the American Experience. In: Reid RL (ed). Indiana University Press, 1-131.
Santos G. (2011) Acid/Base/Acid (ABA) Sample Pretreatment. In: Facility UoCKCCA (ed). University of California Keck Carbon Cycle AMS Facility.
Smith AB and Katz RW. (2013) US billion-dollar weather and climate disasters: data sources, trends, accuracy and biases. *Natural hazards* 67: 387-410.
Stafford CR. (2004) Modeling soil-geomorphic associations and Archaic stratigraphic sequences in the lower Ohio River valley. *Journal of Archaeological Science* 31: 1053-1067.

Stuiver M, Reimer PJ and Reimer RW. (2018) *CALIB 7.1 [WWW program] at* http://calib.org.
Wallace JM and Gutzler DS. (1981) Teleconnections in the geopotential height field during the Northern Hemisphere winter. *Monthly Weather Review* 109: 784-812.
Walthall JA. (1981) *Galena and aboriginal trade in eastern North America*: Springfield, Ill.: Illinois State Museum.
Wright HE, Mann DH and Glaser PH. (1984) Piston corers for peat and lake sediments. *Ecology* 65: 657-659.
Yu B and Zwiers FW. (2007) The impact of combined ENSO and PDO on the PNA climate: a 1,000-year climate modeling study. *Climate Dynamics* 29: 837-851.

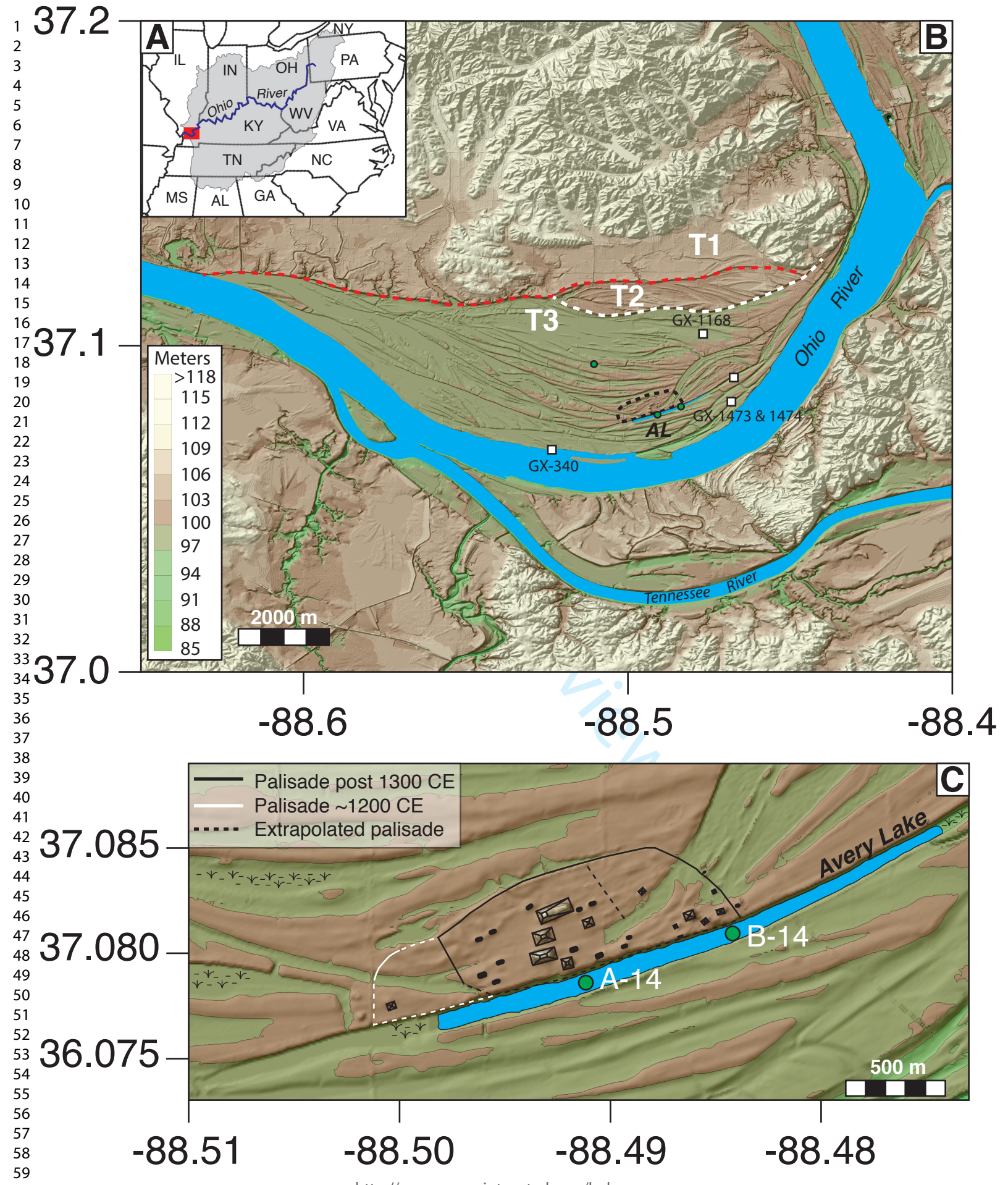

Figure 1: Bird et al., 2018

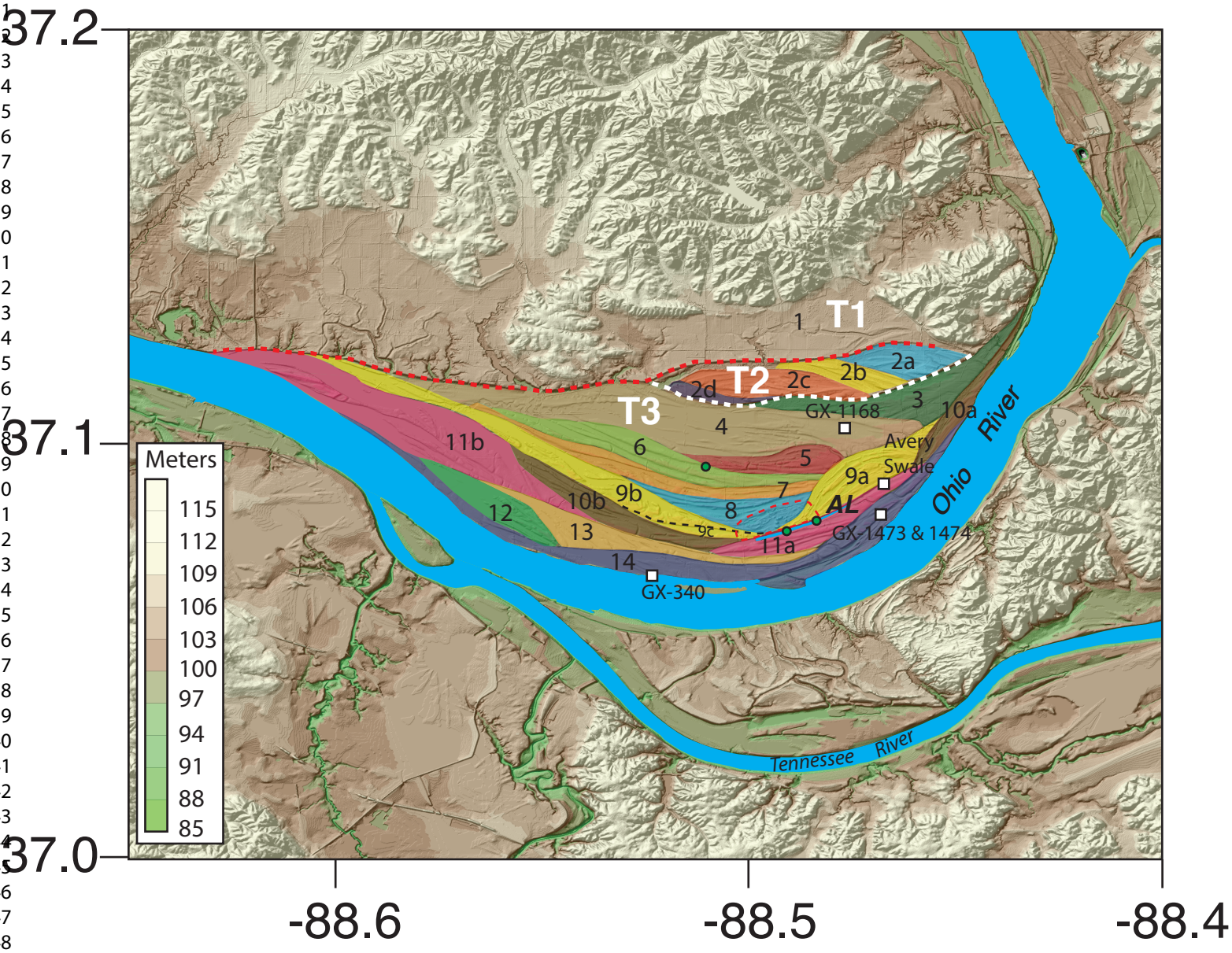

Figure 2: Bird et al., 2018

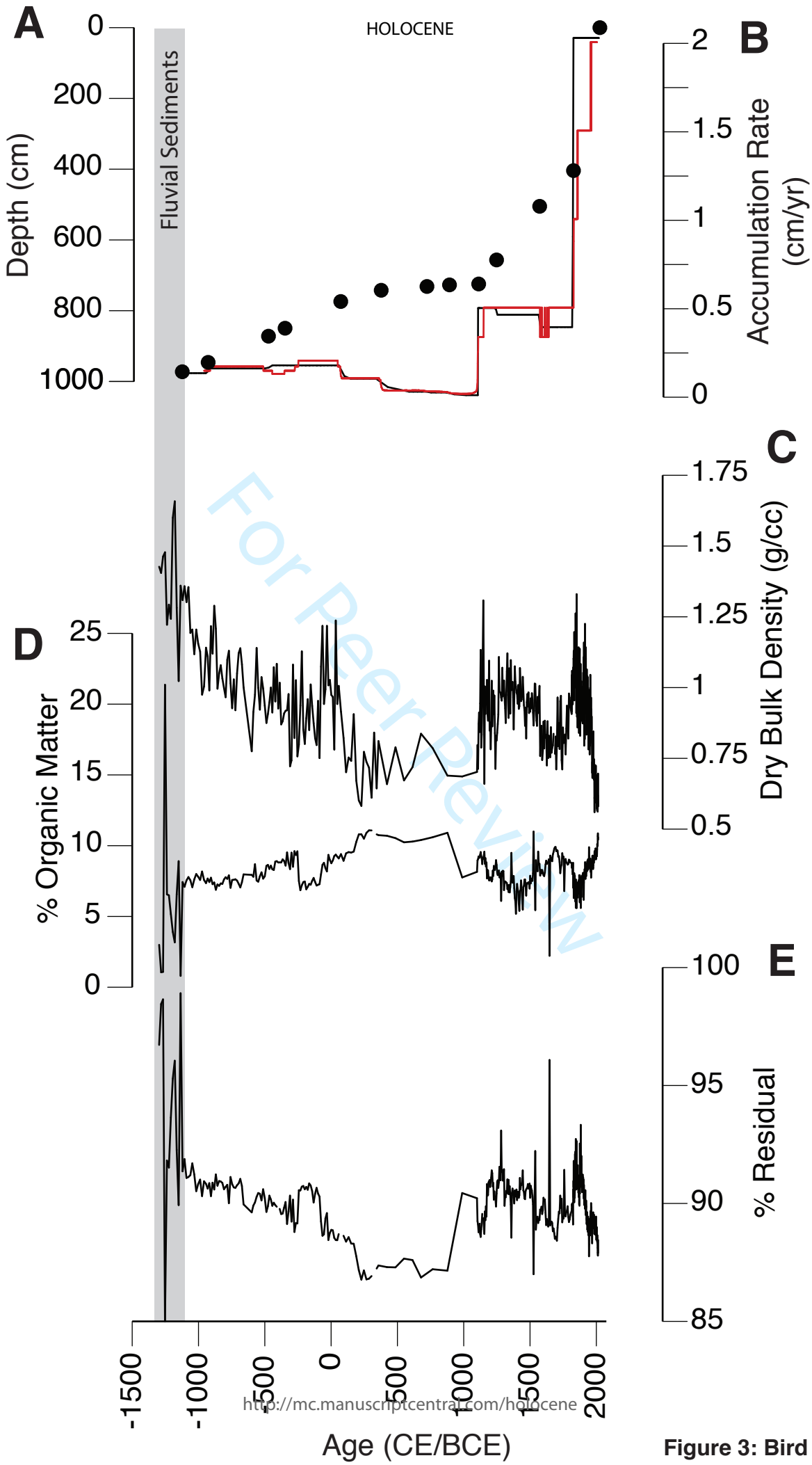

Figure 3: Bird et al., 2018

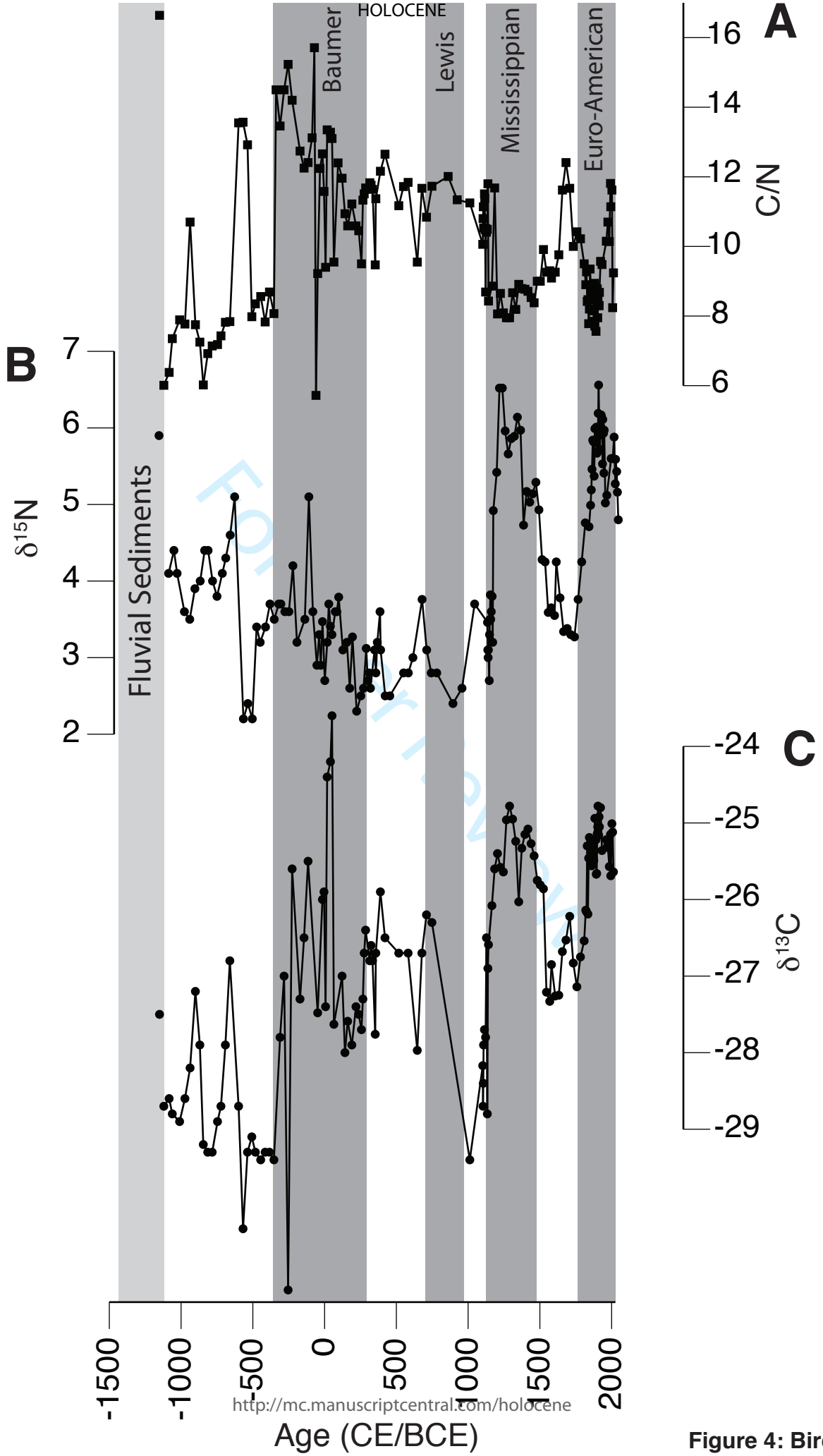

Figure 4: Bird et al., 2018

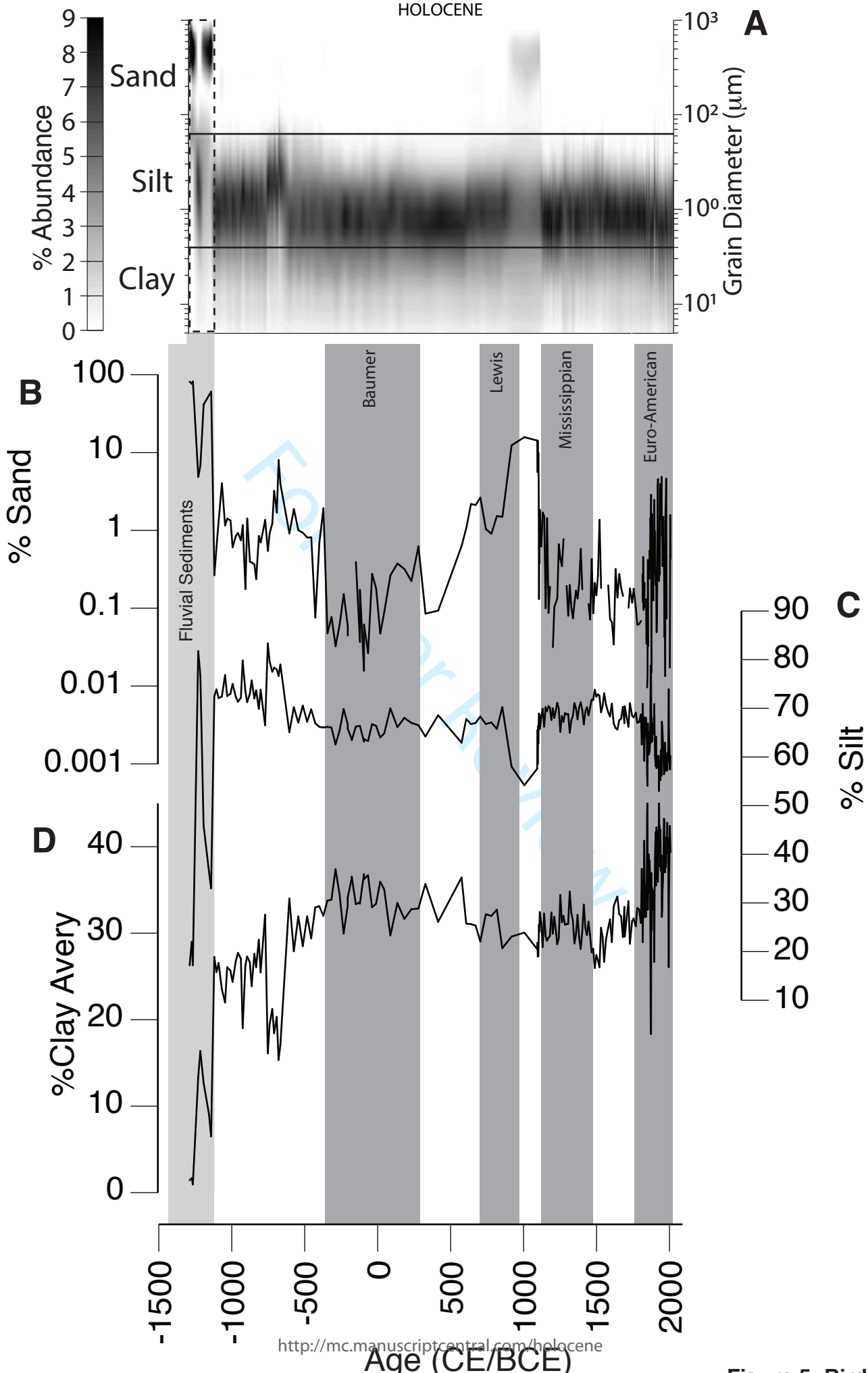

Figure 5: Bird et al., 2018

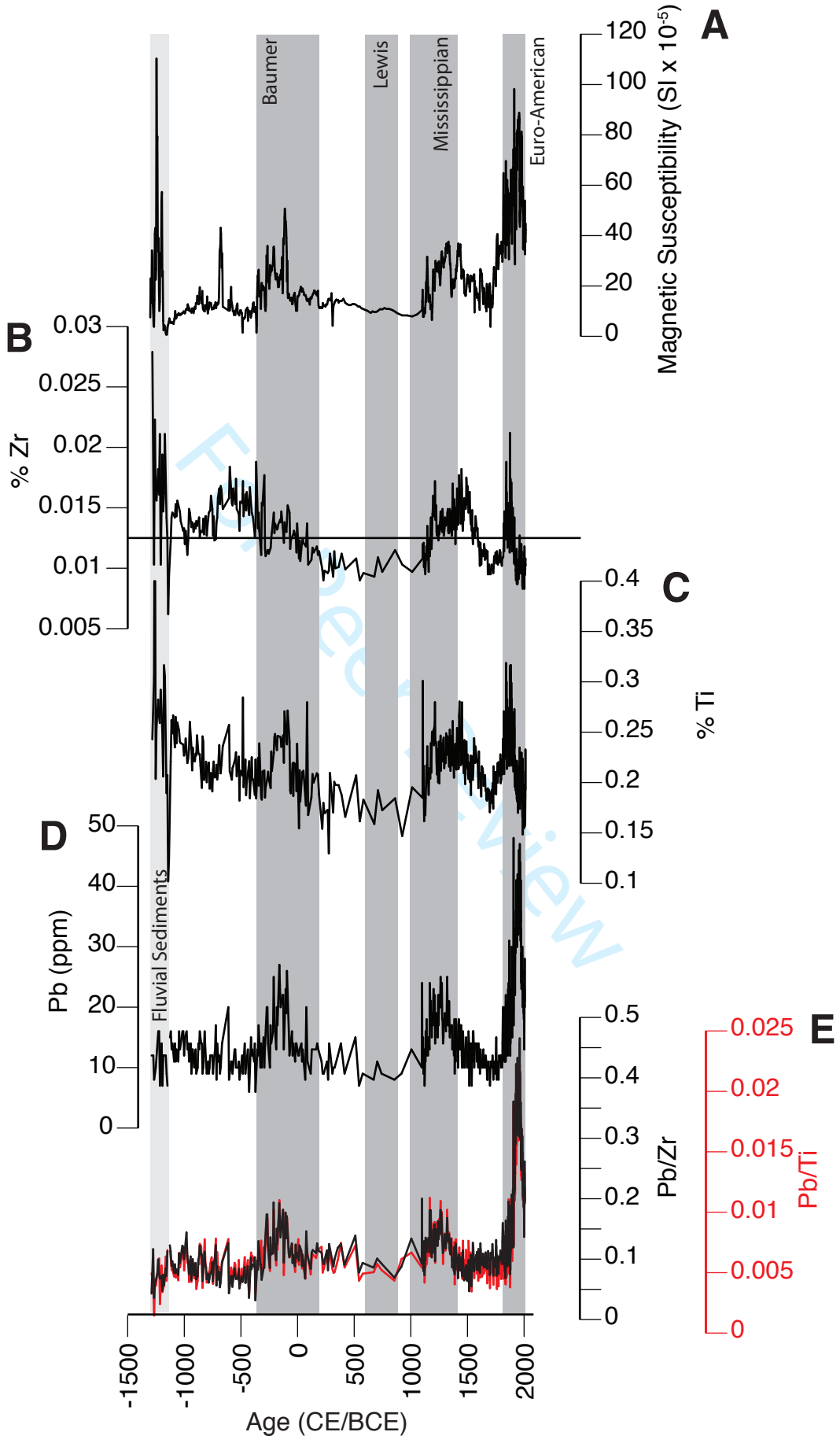

Figure 6: Bird et al., 2018

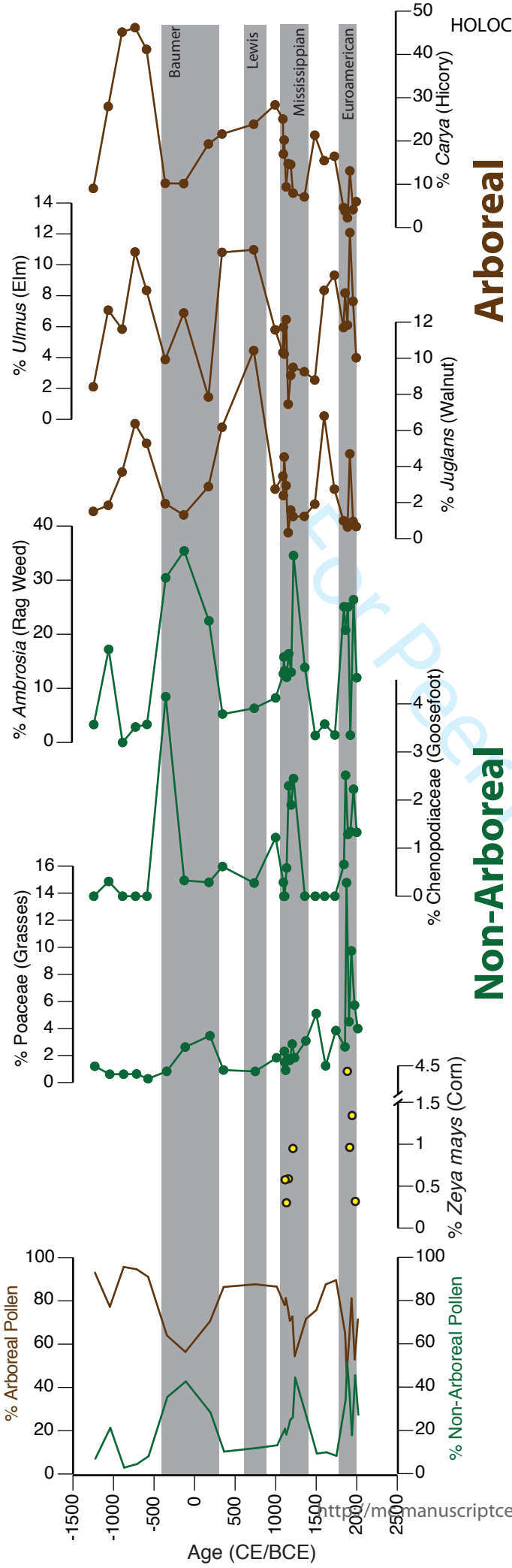

Figure 7: Bird et al., 2018

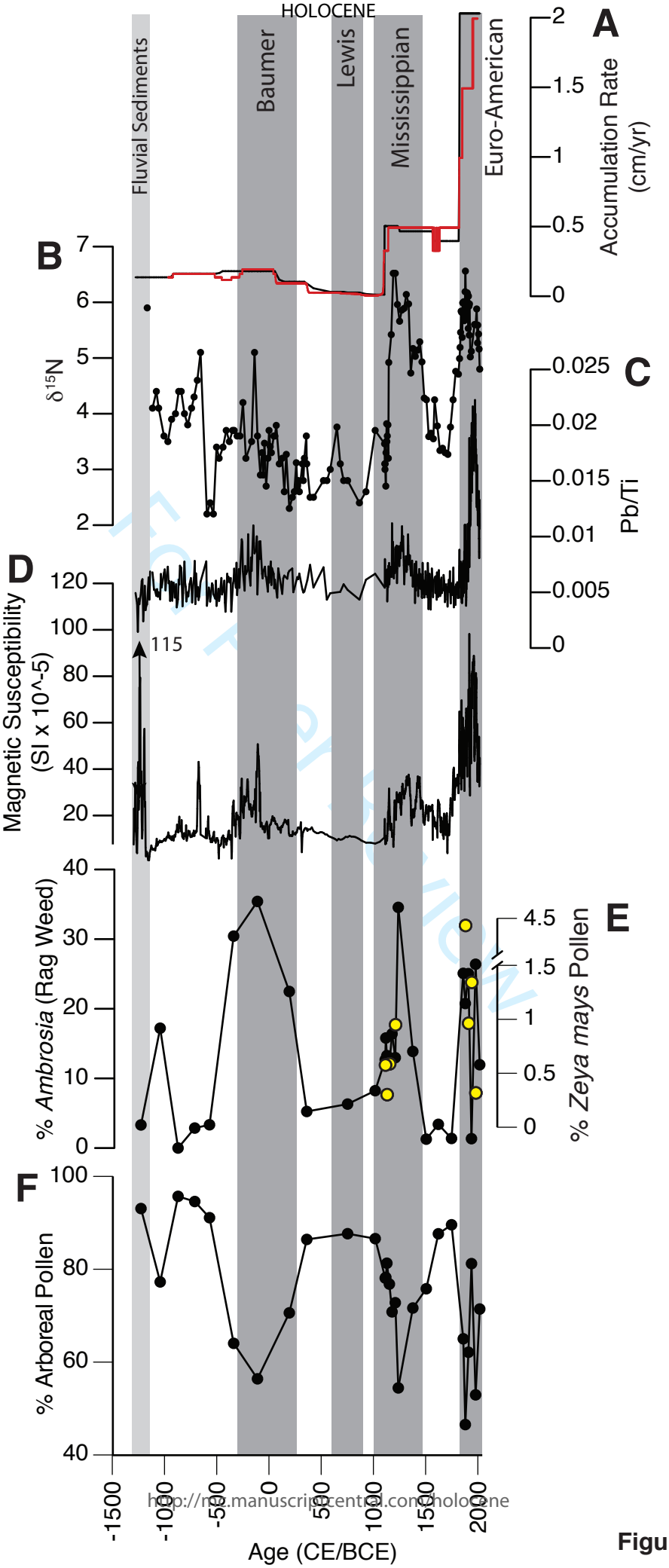

Figure 8: Bird et al., 2018

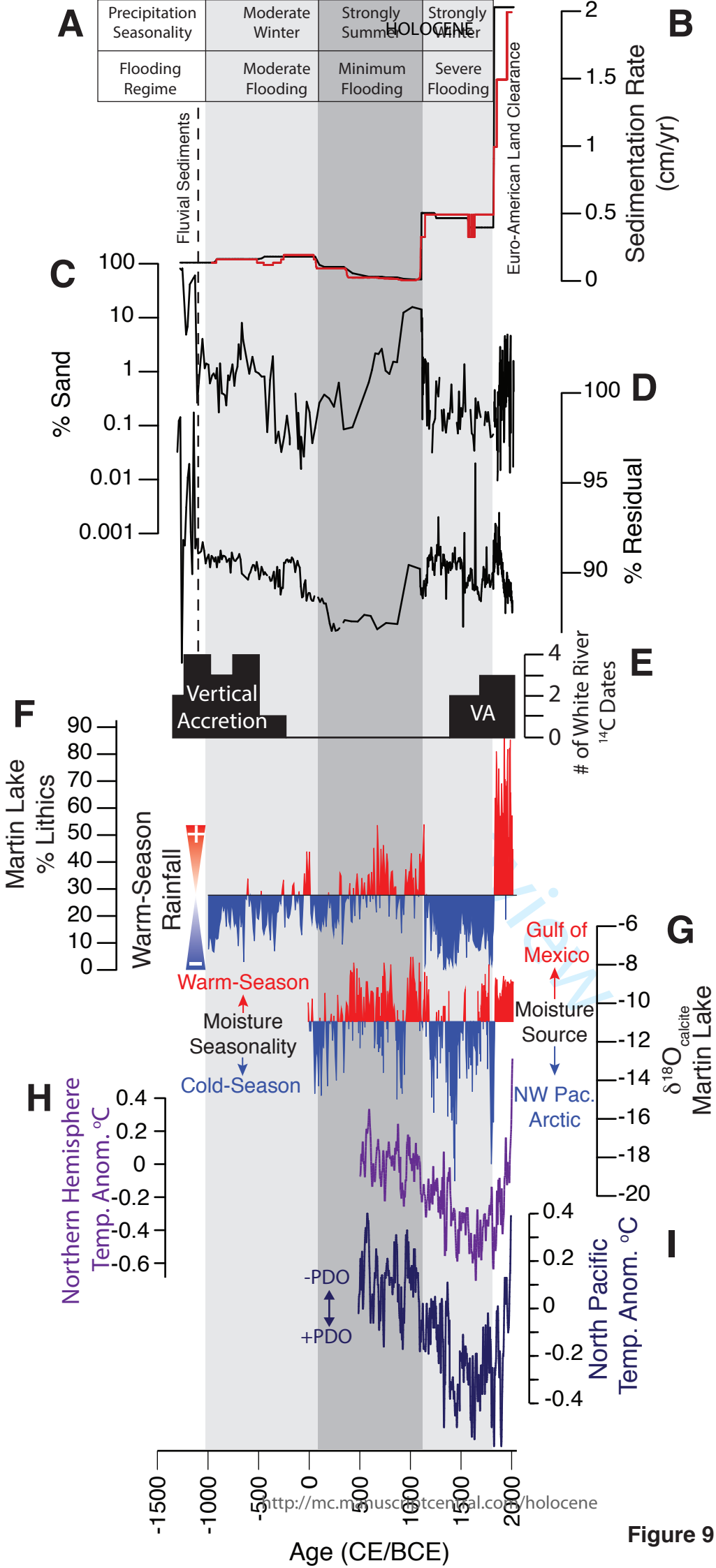

Figure 9: Bird et al., 2018

Table 1 Avery Lake radiocarbon age data.

UCI #	Material	Composite Depth (cm)	^{14}C Age	Error +/-	Median Probability cal yr BP	1 σ Upper Age	1 σ Lower Age	Maximum Probability
145745	Charcoal	404	135	20	130	72	116	0.365
145746	Charcoal	505	315	20	390	375	429	0.782
145747	Charcoal	656.5	805	25	720	693	730	1
145748	Charcoal	724.5	950	20	850	827	864	0.564
182487	Wood	727	1160	15	1070	1054	1085	0.534
180591	Charcoal	731.5	1285	15	1240	1239	1267	0.541
180592	Charcoal	742.25	1685	15	1590	1578	1604	0.633
180593	Charcoal	774	1945	15	1890	1875	1900	0.807
180589	Charcoal	849.5	2260	15	2310	2308	2335	0.746
180590	Charcoal	872	2425	15	2430	2376	2465	0.953
180594	Charcoal	946	2790	15	2890	2859	2890	0.654
145749	Charcoal	972.5	2930	20	3080	3091	3144	0.581